CRREL REPORT 91-10

Impulse Radar Bathymetric Profiling In Weed-Infested Fresh Water

Austin Kovacs

April 1991

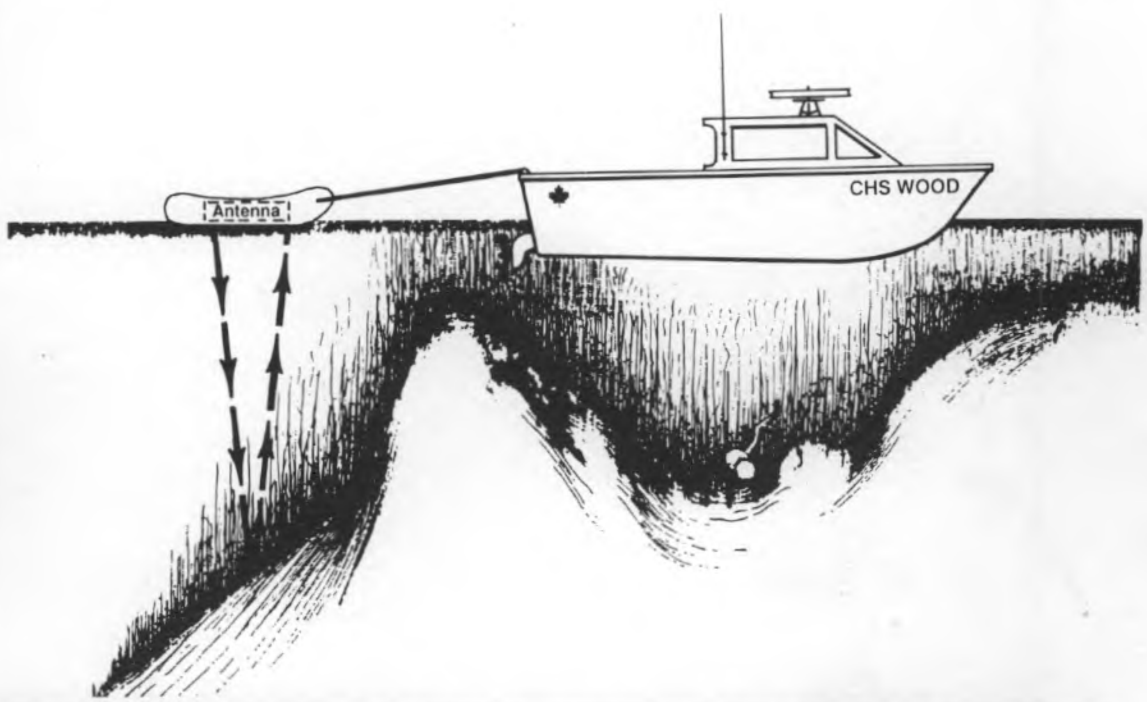

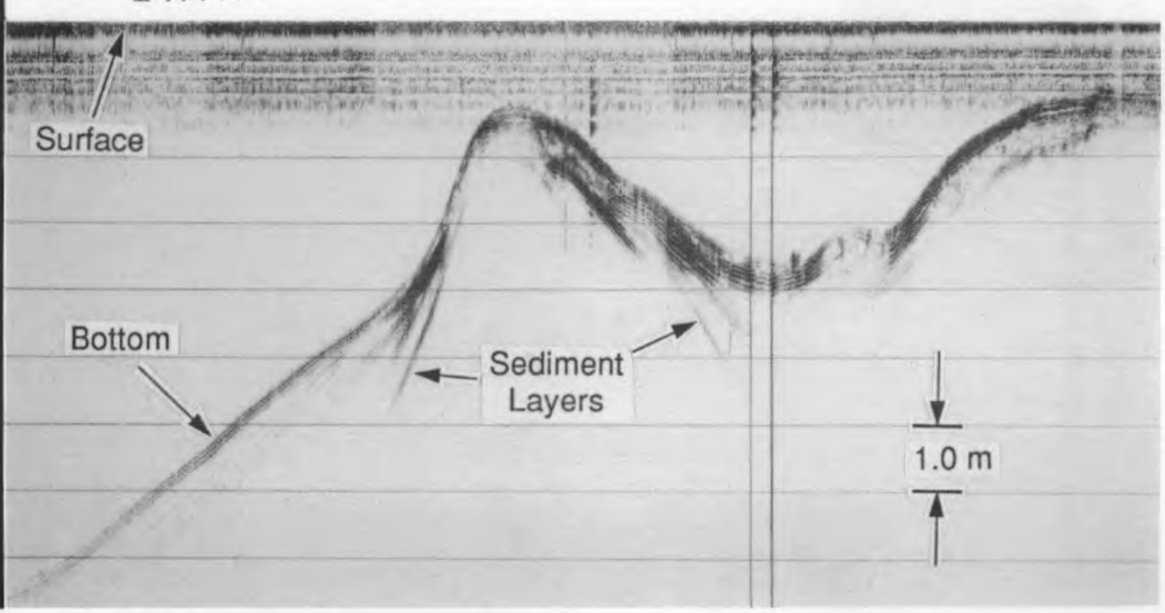

For conversion of SI metric units to U.S./British customary units of measurement consult ASTM Standard E380, Metric Practice Guide, *published by the American Society for Testing and Materials, 1916 Race St., Philadelphia, Pa. 19103.*

COVER: Survey boat configuration and sample radar record.

CRREL Report 91-10

U.S. Army Corps
of Engineers
Cold Regions Research &
Engineering Laboratory

Impulse Radar Bathymetric Profiling In Weed-Infested Fresh Water

Austin Kovacs

April 1991

PREFACE

This report was prepared by Austin Kovacs, Research Civil Engineer, of the Applied Research Branch, Experimental Engineering Division, U.S. Army Cold Regions Research and Engineering Laboratory.

The author wishes to acknowledge the field assistance, during the St. Lawrence Seaway field study, of Michael R. Crutchlow, Dennis A. St. Jacques and Paul G. Millette of the Canadian Hydrographic Service (CHS), Development Division. The author also thanks Greg McKenna of the St. Lawrence Seaway Development Corporation, Marine Yard, Massena, New York, for providing launching and docking facilities for the CHS survey boat, and J. Scott Holladay, of Aerodat Ltd., during the Lake Nipissing survey. The technical advice of Rexford M. Morey on aspects of impulse radar sounding along with his, M.R. Crutchlow's, D.A. St. Jacques' and George Macdonald's review of this report are also acknowledged. Above all, the author again acknowledges M.R. Crutchlow, who was interested in and arranged for the comparative sonar and radar sounding field trials, arranged for reviews of this paper at CHS and provided background material for this paper.

CONTENTS

ILLUSTRATIONS

Impulse Radar Bathymetric Profiling in Weed-Infested Fresh Water

AUSTIN KOVACS

INTRODUCTION

In many rivers and lakes, there is dense vegetation. This growth can reach the water surface and fan out from depths in excess of 3 m. The weeds can make a waterway unnavigable to conventional power boats by fouling propellers. In addition, this growth has prevented bathymetric surveying using acoustic depth sounders operating in about the 100- to 200-kHz frequency band. This inability to obtain depth profiles through dense weed areas along the lakes and riverways of the St. Lawrence Seaway has forced the Canadian Hydrographic Service (CHS) to undertake its shallow-water bathymetric surveys early in the spring, before weed growth prevents acoustic depth sounding, or to make spot tape measurements using a lead line tape. This report presents the results of a test to determine if impulse radar can be used as a depth sounder in the dense weed areas along the St. Lawrence Seaway.

EARLY IMPULSE RADAR USES AND BATHYMETRY STUDIES

The first commercially available impulse radar sounding system was made in 1976 and bought by CRREL from Geophysical Survey Systems, Inc. (GSSI). Prior to this, a prototype system was rented from GSSI and used in 1974 to detect crevasses and profile internal layers and thickness of shelf ice and icebergs in the Antarctic (Kovacs and Abele 1974, Kovacs and Gow 1975, Kovacs 1977a) and subsequently to profile lake ice thickness and under-ice water depth (Kovacs 1978, 1990). Helicopter tests in Alaska also showed that both lake and sea ice thickness and the depth of water under freshwater ice could be profiled from an airborne platform (Kovacs 1977b, Kovacs and Morey 1979, 1980). Many other investigators have since repeated or expanded on these results, not the least of which is the early surface profiling of freshwater ice, frazil ice and sub-ice water depth by Annan and Davis (1977a) and the more recent airborne surveys of the snow depth on ice and the thickness of lake and brackish water ice by Ulriksen (1986). Also of note are the ground-breaking studies at GSSI by Bertram et al. (1972), Orange et al. (1973), and Morey et al. (1973) on impulse radar sounding of lake and sea ice thickness, freshwater bathymetry, and permafrost features.

Impulse radar was also used by GSSI staff in 1975 to profile sludge sediments, with methane gas inclusions, in the Charles River, Boston, Massachusetts.* At the time, Professor Albert Edgerton, of the Massachusetts Institute of Technology, was attempting, without success, to profile the thickness of the sediments using a variety of acoustic sounding techniques. The impulse radar successfully profiled both the top and bottom of this gaseous sludge fill, allowing an estimate to be made of the amount of sludge material to be removed by a Corps of Engineers dredging contractor. In addition, impulse radar was used in the mid 1970's by Morey* to profile the thickness of a layer of sunken logs near a paper mill in the St. James River, Maine, and to detect logs floating below the water surface. An acoustic sounder was also tried for sounding the log layer thickness but without success.

It was the success of these early surveys as well as the demonstrated capability to profile the depth variation and internal structure of snow, sand and other air entrained materials that gave us reason to believe that impulse radar could provide bathymetric profiles in weed-infested waters where acoustic sounders could not.

OPERATING PRINCIPLES

Ground-penetrating impulse radar sounding systems typically operate in the VHF and UHF frequency bands (between 30 MHz and 3 GHz), where 300 MHz is the frequency separating the two bands. In GSSI systems, an impulse of electromagnetic energy of a few nanosec-

*Personal communication with Rexford M. Morey, 1990.

onds duration is transmitted from an antenna into a material. The transmitted wavelet has a broad band with a frequency bandwidth on the order of 100 MHz at the –3 dB power level. The center frequency of the transmitted wavelet spectrum and the time duration of the emitted energy in air are functions of the size of the antenna and its dampening characteristics as well as the impulse transmitter characteristics. Where the electromagnetic energy is radiated from an antenna into a material and impinges on a horizon or object of dielectric contrast, a portion of the energy will be reflected. The amount of energy reflected back to the receiver will depend on the distance and the size, roughness and slope of the target, as well as the electrical contrast at the interface. The energy not reflected back may be scattered or will continue onward where the process may be repeated or until the energy is completely attenuated. The depth of penetration is dependent on the electrical properties of the subsurface materials—for example, the relative dielectric constant, which governs the wavelet velocity; the conductivity, which governs energy attenuation; and on-beam spreading losses. The reflected energy sensed by the receiver is frequently displayed in real time on a graphic recorder, in a manner similar to a time-domain acoustic sub-bottom sounding system used to profile marine sediment layers. This is how the impulse radar system was used in this field study. The data may also be displayed in real time on a color cathod-ray tube display or stored on magnetic tape for later playback and analysis. The primary quantity measured is the two-way travel time between various targets or subsurface interfaces.

THEORETICAL CONSIDERATIONS

The effective wavelet propagation velocity, V, of the transmitted electromagnetic pulse in a medium can be calculated from

$$V = \frac{c}{\sqrt{\varepsilon' \mu_r}} \tag{1}$$

where c = electromagnetic wave velocity in air (~0.3 m/ns)

ε' = real dielectric constant of the medium

μ_r = relative magnetic permeability (unity for non-magnetic materials).

Depth, D, can be estimated from

$$D = \sqrt{\left(\frac{t_D V}{2}\right)^2 - \frac{S^2}{4}} \tag{2}$$

where t_D = wavelet travel time from the surface to some sub-bottom interface and return

S = separation distance between transmit and receive antennas.

Where a single transceiver antenna is used, this equation reduces to

$$D = \frac{t_D V}{2} . \tag{3}$$

The relative dielectric constant of many materials is frequency- and temperature-dependent. For example, in the UHF frequency band, water at 0°C has an ε' of 88 where as at 25°C it is ~80. During any bathymetric survey, it is unlikely that water temperature will vary significantly and thus adversely affect the sounding results. As an example, for a temperature change from 20 to 15°C, the real part of the dielectric constant, which affects wavelet velocity (eq 1), of freshwater would increase by about 1% at the frequencies of interest. This would decrease the wavelet velocity by 0.0002 m/ns. Therefore, once the radar is calibrated, the soundings should be very accurate, all other conditions being equal.

For most materials in situ, a best-guess estimate of ε' is often used to determine the wavelet velocity. However, where borehole information exists on the depth to subsurface layers or the depth of water is accurately known at a calibration site, this information can be used to determine V and ε' using the above equations, or it can be converted into a depth scale on the graphic recorder.

Past experience with GSSI impulse radar systems revealed that they can be affected by temperature variations, probably because mil. spec. electrical devices are not used. A sudden, large temperature change may cause drift in the time base, which could adversely affect the sounding results. Therefore, after initial calibration, the radar console should be protected from sudden or large temperature changes.

GSSI antennas transmit a conical beam. The –3-dB width in air is approximately 90° perpendicular to the antenna electric (E) field and about 80° parallel to the E field. For most surveys and in particular for shallow sounding in low-loss materials, the footprint can be considered circular and may be determined by $2 \sin^{-1} (1/\varepsilon')$, where ε' is the real part of the complex dielectric constant. Since ε' is 1 in air, the calculated beam-width is then 90° and when the antenna is in contact with fresh water, which has an ε' of ~81 at 20°C, the beam-width narrows to about 12°. For shallow water surveys (less than 5 m), where the antenna is resting on the water surface, a reasonable approximation of the beam radius R is $R = 0.1D$, where D is the water depth. Therefore, for

2-m-deep water, the beam diameter would be about 0.4 m.

Further narrowing of the beam width can be achieved by lifting the antenna above the surface. To produce the minimum beam width in water, one needs to raise the antenna ~$0.1 \times \lambda$, where λ is the length of the transmitted wavelet's center frequency in air. Therefore, at 300 MHz where λ is 1 m, the antenna should be elevated about 0.1 m above the water surface to achieve a minimum footprint. However, there are other effects to consider, especially that related to energy transfer. To maximize energy transfer, the antenna should be placed on the water surface. For a more complete discussion of the above topics, consult the reports by Smith (1984) and Smith and Scott (1989).

A factor that may on occasion be important is the radiated beam "cone" angle in water versus bottom slope. As the antenna approaches a steeply shoaling area, the forward edge of the beam "sees" the bottom first. The related two-way slant-range travel time to this location, as displayed on the graphic record, will therefore indicate a depth somewhat less than that which exists directly below the antenna. The variation from the true depth below the antenna will depend upon cone angle, bottom slope and the slant range. For shallow bathymetric surveys, such as in weed-infested waters, this effect should not be of consequence. In deep water with abrupt bottom variation, a comparative bathymetric survey using the impulse radar and an acoustic sounder would be desirable, in lieu of simple but not necessarily appropriate calculations, for assessing sounder depth differences, if any. Using separate transmitter and receiver antennas would certainly aggravate this sounding situation and should be avoided.

When an antenna is placed on water or on any material, there is an impedance loading associated with the dielectric properties of the material. This loading reduces the center frequency of the radiated wavelet. For example, Kovacs and Morey (1985) found the following from transmission studies using borehole antennas. In air the center frequency of the wavelet spectrum at the receive antenna was about 140 MHz. When the transmit and receive antennas were placed in separate boreholes spaced about 5 m apart in ice with an apparent dielectric constant of 3.15, the transmitted wavelet recorded at the receiver had a center frequency of about 111 MHz. Disregarding any frequency-dependent attenuation effects, the result of antenna loading was a reduction in the transmitted wavelet center frequency of about 20%. In another test where the antennas were placed in –0.25°C water with an apparent dielectric constant of 88, the center frequency of the received wavelet was 104 MHz or about 25% less than the free-space value.

Another indication of the effect of antenna loading was demonstrated during a test conducted by Kovacs and Morey (1980) where a GSSI Model 3105 (300-MHz) antenna was used to sound sea ice thickness both from the surface and from a platform. The free-space center frequency of the wavelet spectrum transmitted by this antenna was found to be 280 MHz. When the antenna was placed on the sea ice, the center frequency of the reflected wavelet from the ice bottom was 131 MHz vs 174 MHz when the antenna was elevated about 1.7 m above the surface. Here the frequency-dependent attenuation of the ice, the ice bottom roughness characteristics, and the electromagnetic properties of the reflective boundary were not changed. Impedance loading did occur when the antenna was on the ice, and this caused a 25% decrease in the center frequency of the reflected wavelet.

Based on the above findings, it is reasonable to expect that, for a GSSI antenna resting on fresh water, impedance loading will reduce the center frequency of the transmitted wavelet by about 25% from the free space value. The reduction will be dependent on parameters related to the antenna housing and the medium (air, wood, rubber, etc.) between the housing and the water. In short, a GSSI antenna's radiating element is seldom in direct contact with the medium being sounded. In addition, a further reduction in the center frequency will occur with increasing water conductivity and depth (Wensink et al. 1990), since the higher frequencies are attenuated in a conductive medium. Therefore, the reduction in center frequency noted above could indeed be larger.

Another parameter that may be estimated is the wavelength of the wavelet's center frequency in water. If an antenna, with a transmitted center frequency of 300 MHz in air, is set on water, impedance loading may reduce the center frequency of the radiated wavelet by about 25% to 225 MHz. At 225 MHz the wavelength $\lambda = C/f$ where C is the velocity of light in air (300 m/μs) and f is the impulse wavelet's center frequency (MHz). Therefore, the radiated wavelength is ~1.33 m, but as the wavelet travels into the water it reduces to λ/ε or to ~0.15 m. The effect of these reductions should be an increase in sounding depth and increased resolution since objects on the order of one-half the wavelength should be detectable.

Annan and Davis (1977b) modified the radar range equation to take into account the effect of electromagnetic attenuation in conductive materials. Their formulations were used to estimate the sounding depth of the impulse radar in water vs water conductivity (Fig. 1). In

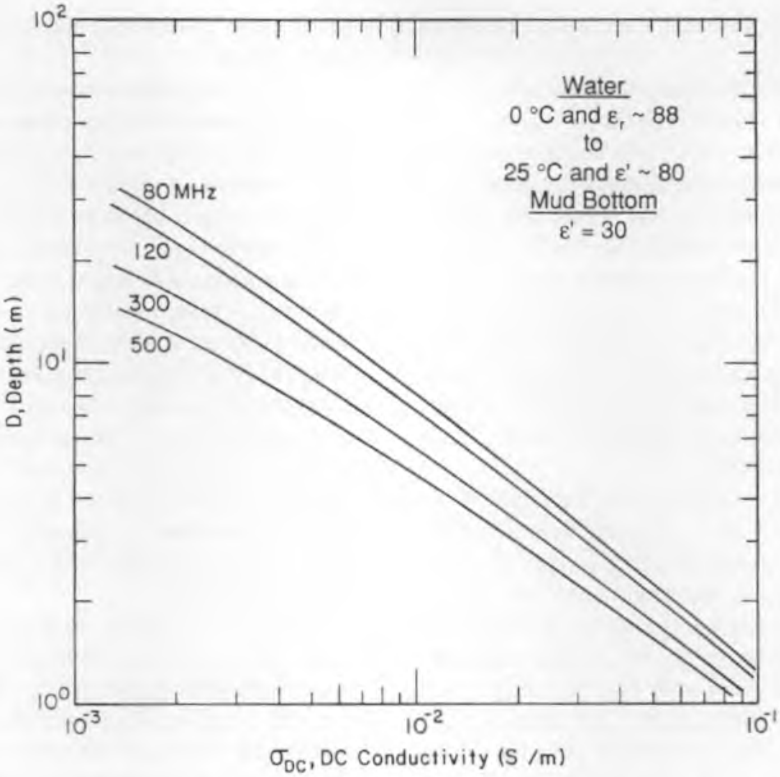

Figure 1. Estimated impulse radar sounding depth vs water conductivity with transmitted wavelet center frequency in water as a parameter.

the analysis a smooth mud bottom with a relative dielectric constant of 30 was used. The curves shown in Figure 1 are representative for the wavelet center frequencies shown and water temperatures between about 0 and 25°C. The conductivity of the water at our study sites at the western end of Lake St. Francis, St. Lawrence Seaway, was measured to be 3.1 mS/m. Therefore, at 100 MHz, the impulse radar should be capable of profiling the bottom to a depth on the order of 19 m while at 400 MHz this depth would be about 7 m less. It should be clear from Figure 1 that impulse radar depth sounding in water with a conductivity greater that 0.1 S/m is extremely range limited and is of no practical value in seawater.

STUDY AREAS

Impulse radar soundings of water were made at three sites. Initial tests were made in the Grass River, which runs through Massena, New York, and discharges into the St. Lawrence River just below Snell Lock, to confirm the operation of both the GSSI System 3 impulse radar and the Ross 801 precision acoustic depth sounder (sonar) systems used. In this water course, thick weed growth was found near the river banks and on shoal areas.

The second and most important site was along the western edge of Grass Island near FIG buoy D81. This location is circled in Figure 2. At this site there was dense weed growth up to 3 m thick. Three different varieties were harvested (Fig. 3). Milfoil, which has finely divided leaves, is at the top of the photo. To the left is a broadleaf weed and on the right is a long, stringy water grass. At this site, portions of the weeds not only reached the water's surface but grew to such lengths that they streamed with the current for a meter and more along the surface (Fig. 4 and 5).

The last site was near South Lancaster, Canada. Here the weed growth generally did not reach the surface but it was very dense.

Figure 2. Location of Grass Island beside the St. Lawrence Seaway ship route. Lake St. Francis extends eastward from Grass Island. All colored water areas have mild to dense weed growth where water depths cannot be profiled with conventional acoustic depth sounding systems.

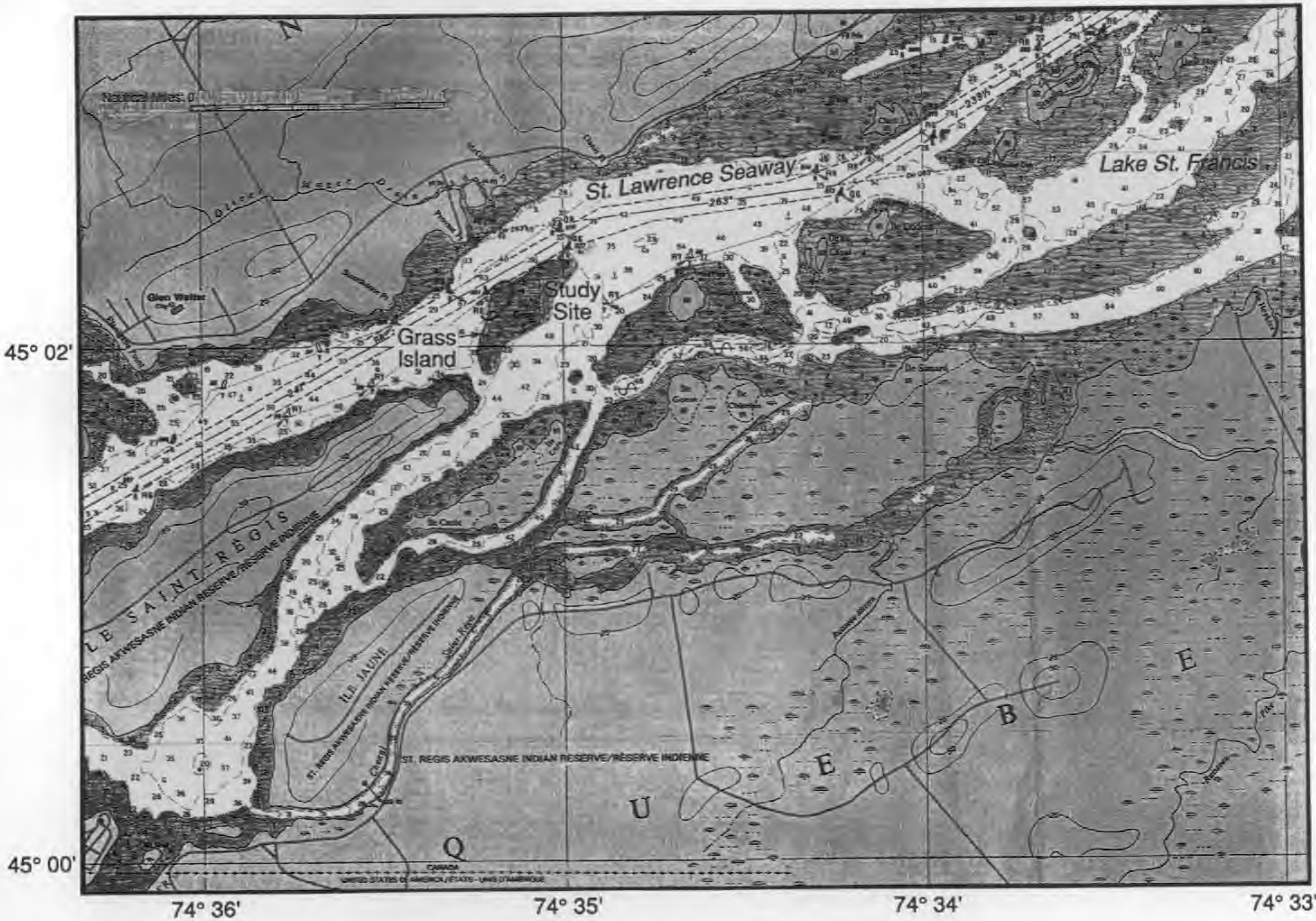

St. Lawrence Seaway
Lake St. Francis
Study Site
Grass Island
Glen Walter
ILE SAINT-RÉGIS
ST. REGIS AKWESASNE INDIAN RESERVE/RÉSERVE INDIENNE
ILE JAUNE
Q U E B E C
CANADA
UNITED STATES OF AMERICA / ÉTATS - UNIS D'AMÉRIQUE
45° 02'
45° 00'
74° 36'
74° 35'
74° 34'
74° 33'

Figure 3. Vegetation pulled from the water at Grass Island. The more abundant variety was milfoil (top of photo).

Figure 4. Vegetation growth off Grass Island.

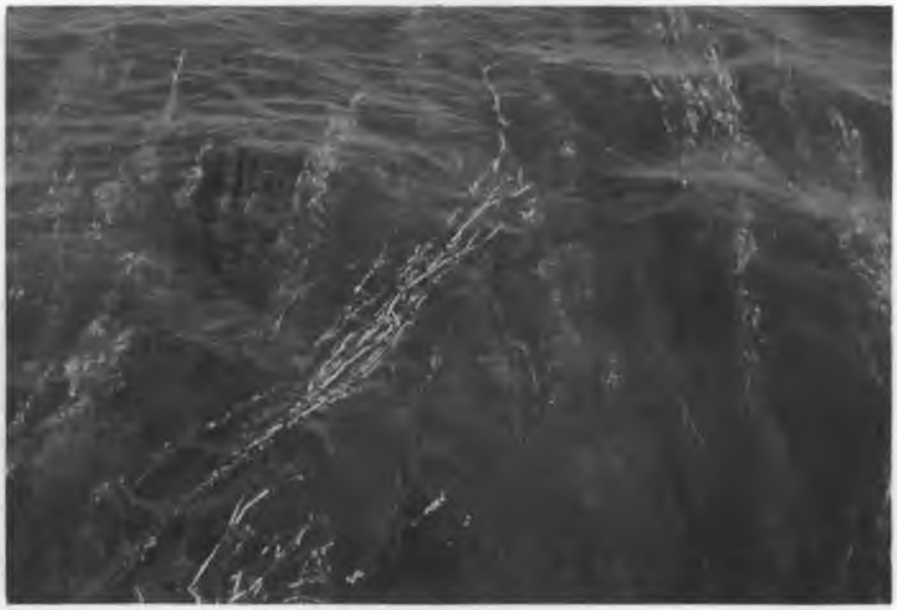

Figure 5. Long weeds bent by the current off Grass Island.

OPERATIONS

A CHS fiberglass boat was used for the field test. Mounted in the bottom of this 7-m-long vessel was the acoustic transducer for the sonar system. An inflatable rubber boat was used to carry the GSSI 120-, 300- and 500-MHz antennas, one at a time. The 300-MHz and 120-MHz antennas are shown installed in the rubber boat in Figure 6. The inflatable boat was towed about 2 m behind the survey boat. This distance and the use of a rubber boat provided adequate antenna isolation to prevent recording of reflections from metal objects, namely in the survey boat. Some unwanted electronic noise was recorded, which produced some horizontal banding through the radar's graphic record.

In addition to the antennas, the radar system included a graphic recorder with built-in radar controller electronics (Fig. 7). This unit was operated from the back deck of the survey boat. The radar system is configured to run on 20 to 32 V DC or 115 V AC current. In this study the unit was powered by a small gas generator, also set on the back deck of the boat.

During the course of the evaluation, the sonar record was used for comparison with the radar record. A lead line measurement was used to provide depth information for calibrating both sounding systems. Lead line measurements were also used to verify the radar system's depth results where thick weed growth prevented the bottom from being profiled with the sonar system.

RESULTS

Two examples of the radar and sonar records obtained on the Grass River are shown in Figure 8. The radar records were obtained with the 120-MHz antenna. The vertical hatch on the radar record shown in Figure 8 was caused by excessive amplifier gain. This figure shows that the radar system not only provided a good profile of the river bottom but also showed a sub-bottom layer as well as an indication of fish at a depth of about 3.3 and 4 m.

It should be pointed out that the radar antenna was some 4 to 5 m behind the sonar transducer. When the survey boat was under way, both sounders would profile the same track line, but when the boat was allowed to drift over a shoal, such as in Figure 8, the antenna and transducer may not have passed over the very same track.

The sonar record in Figure 8a shows specular noise in the first 2 to 3 m of depth. This probably is attributable to electronic noise produced by the recording system.

Both sounding systems provided good depth information, except over the shoal where the sonar system profiled the top of the weeds. This effect is much more apparent in Figure 9, where the sonar record again shows no bottom information in the shallow shoal area, whereas the radar record clearly shows the bottom. The radar system's depth was verified by lead line sounding. Note also the significant riverbed roughness (shown in

a. 120 MHz.

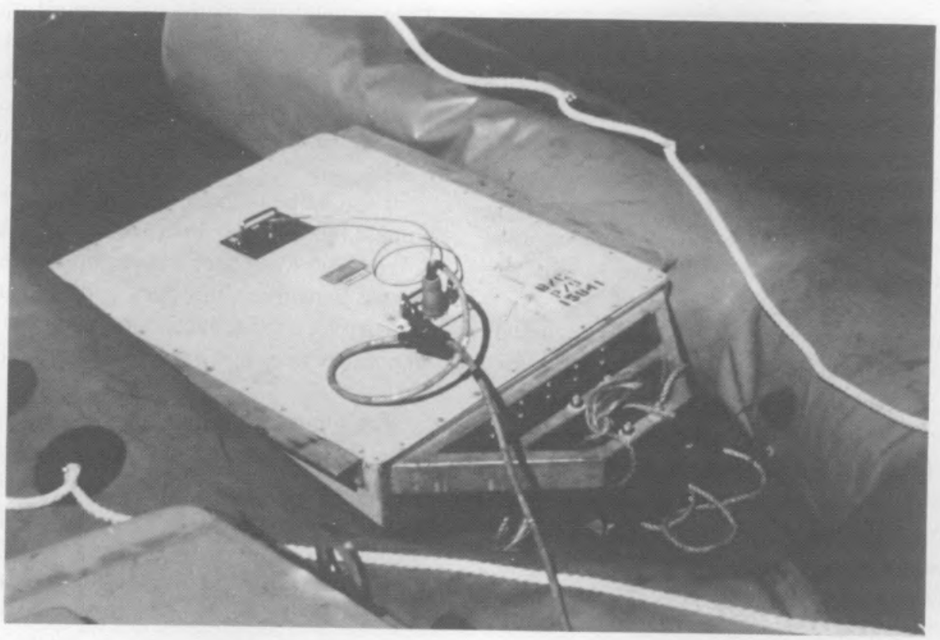

b. 300 MHz.

Figure 6. Placement of the antennas in rubber boat.

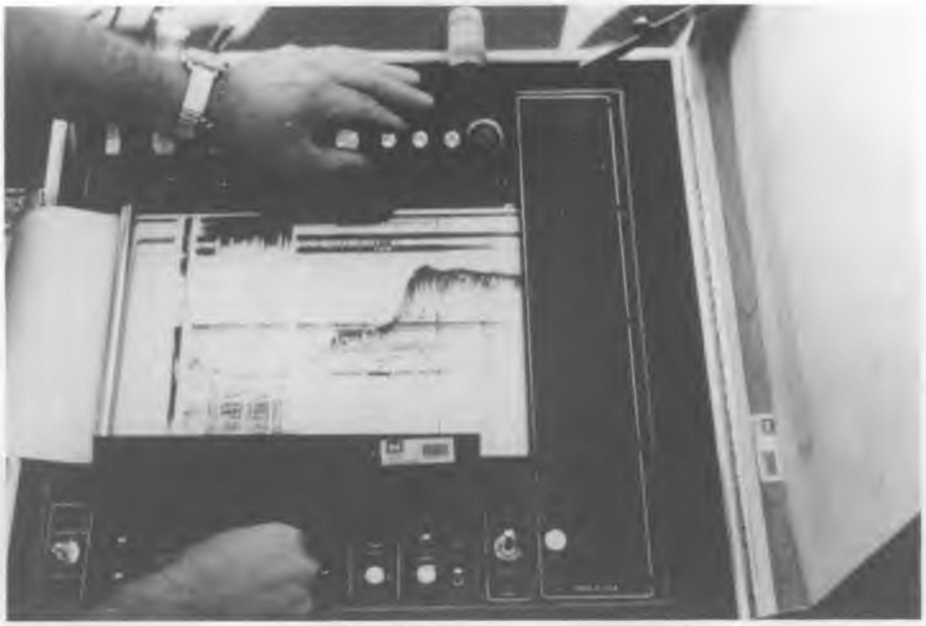

Figure 7. GSSI System 3 recorder–radar controller being adjusted prior to a sounding run off Grass Island.

both records) to the left of the shoal. While this bottom relief was not observed at any other location, it does allow a subjective comparison of the resolution of the two systems to be made. For the conditions at this site, it would appear that the two systems provided very similar micro-scale relief information.

The deepest water encountered in the Grass River was about 9 m; the radar provided good bottom profiles at this depth.

Following the trials with the 120-MHz antenna, the shorter wavelength, higher resolution 300- and 500-MHz antennas were used. The 500-MHz antenna provided depths to about 6 m, while the 300-MHz antenna was not depth-limited in these waters.

At Grass Island (Fig. 2) radar profiles were made using the 300-MHz antenna. Two example records showing a comparison between the radar and sonar profiles obtained are given in Figures 9 and 10. These figures clearly show that the sonar system was unable to penetrate the weeds but did provide the depth to the top of the weed layer. The sonar system lost bottom return in water 2 to 2.5 m deep where the weeds reach some critical density. At this weed density the transmitted acoustic energy could no longer reach the bottom, or the reflected energy from the bottom was scattered or otherwise attenuated and could no longer be detected at the receiver.

An interesting bottom return, shown in the radar record in Figure 9, is the one labeled "fluff layer." This deep water area was near the shipping lane and may represent a loose sediment layer or one referred to in the dredging industry as a fluid mud suspension. This material, as found in many shipping channels, has a specific gravity between 1.05 and 1.3. In any event, the sonar record shows the top of this material, while the radar record also reveals a higher impedance interface below the river bottom that could be bedrock.

Another interesting aspect of the Figure 9 radar record is the sediment layers below the shoal surface. Since this area has very dense vegetation growth, it is reasonable that the sediments are composed, in part, of decaying plant matter. This would imply that there may be methane gas entrapped in the sediments. In this type of sediment, sub-bottom acoustic profilers do not work because the gas inclusions scatter and attenuate the acoustic energy. Similar to its ability to penetrate the weeds, the radar was not affected by any gas inclusions that may have existed in the sediments and did reveal layers in the sediment. Deeper layers would have been detected in the sediment had a lower frequency antenna been used.

The radar and sonar records in Figure 10 again reveal that the sonar system lost bottom return at about the 2.5-m depth on the left end of the record and did not record a bottom where the radar record shows about 2.8 m of water. At this location the sonar system was profiling the top of the weeds, which were about 1.5 m below the surface.

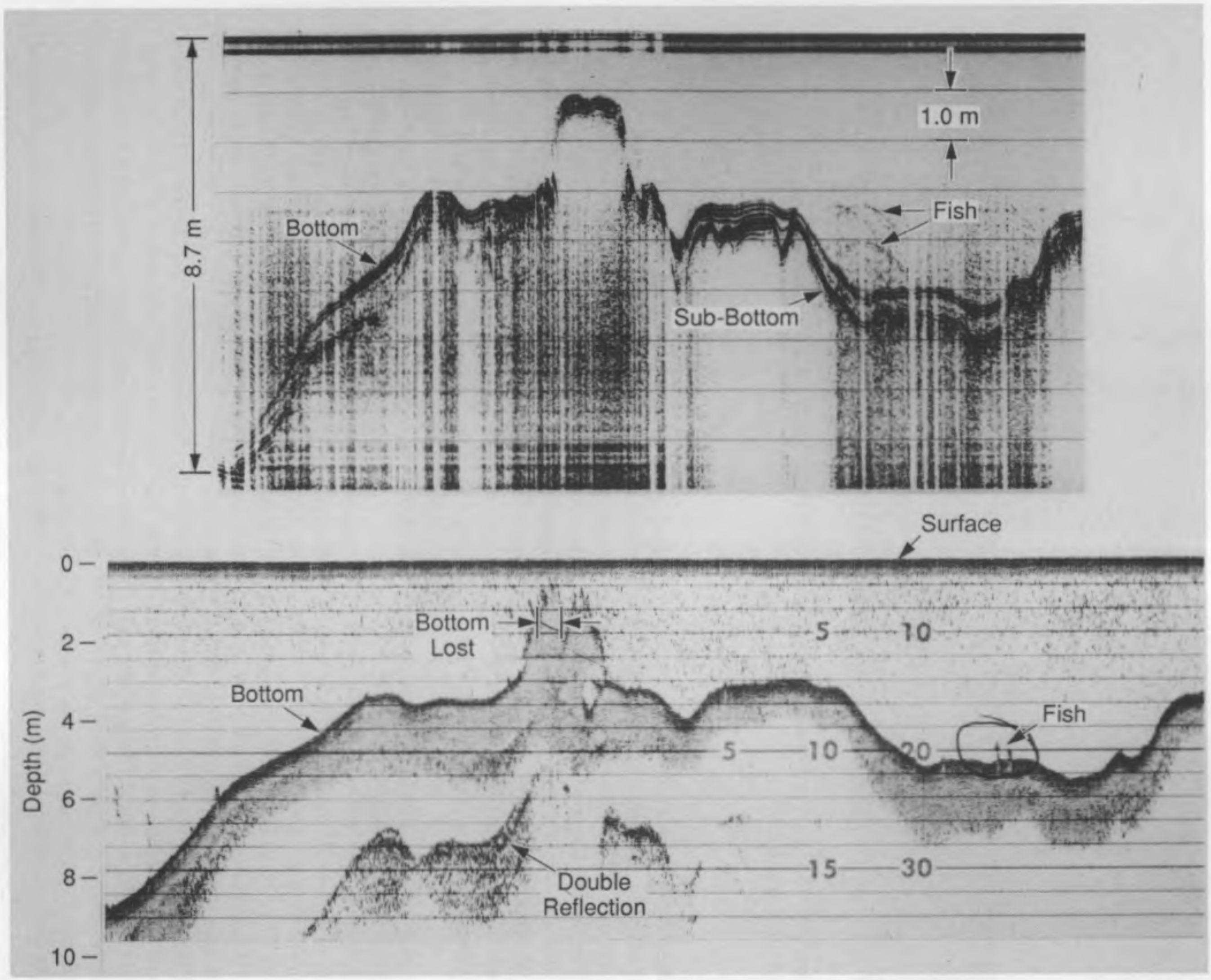

a. Note the sub-bottom reflection and hyperbolic fish signature in the radar record. The fish would be located at the top of the hyperbolic signature. Dark, vertical hash is noise in the radar record as are the spots in the sonar record. The sonar did not give correct water depth in the weeds on the shoal.

Figure 8. Radar (upper) and sonar (lower) profiles obtained in the Grass River.

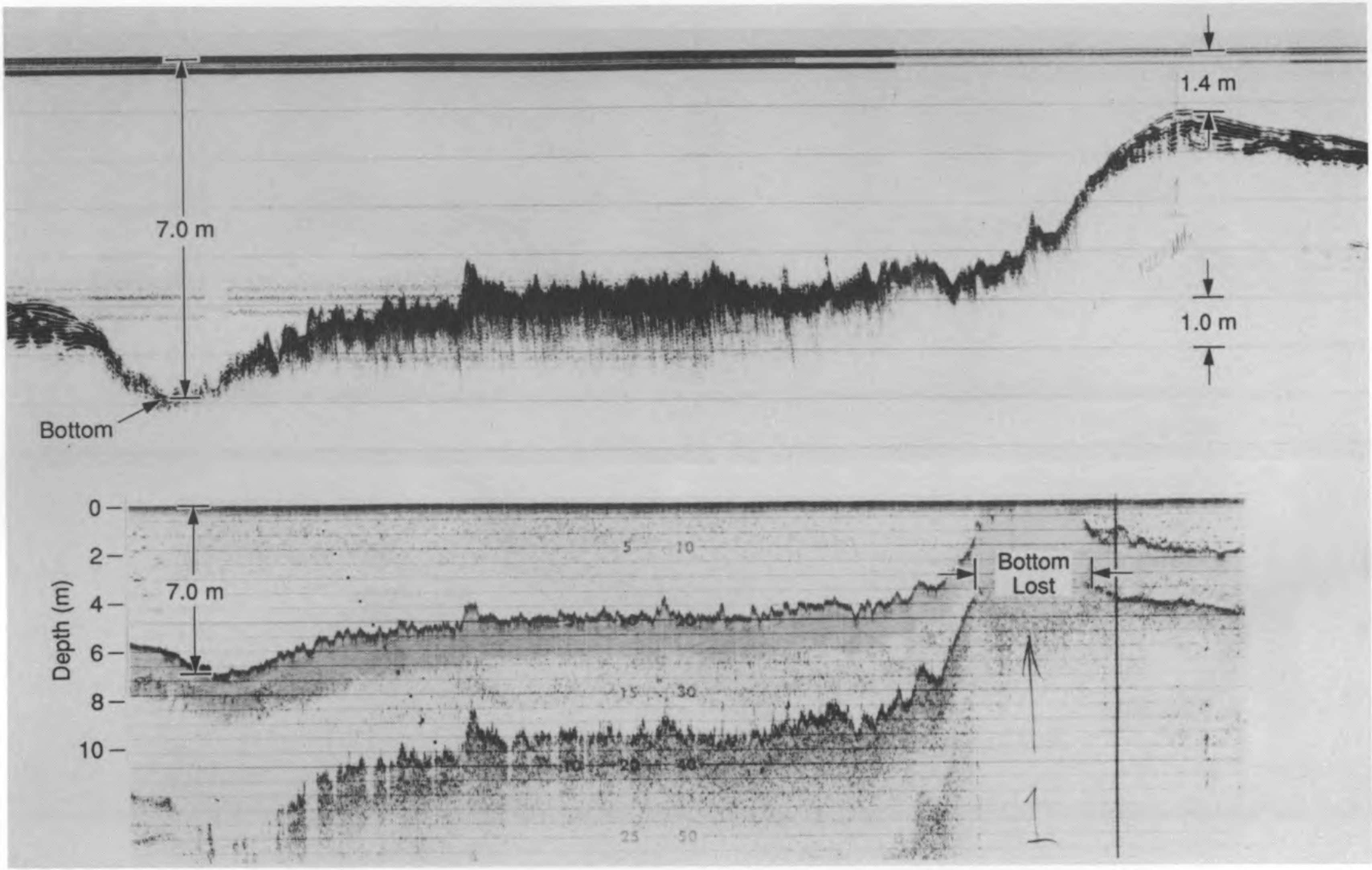

b. The sonar lost bottom-return at a depth of about 2 m at the shoal but did profile the top of the weeds. Note the bed roughness in both records to the left of the shoal.

Figure 8(cont'd). Radar (upper) and sonar (lower) profiles obtained in the Grass River.

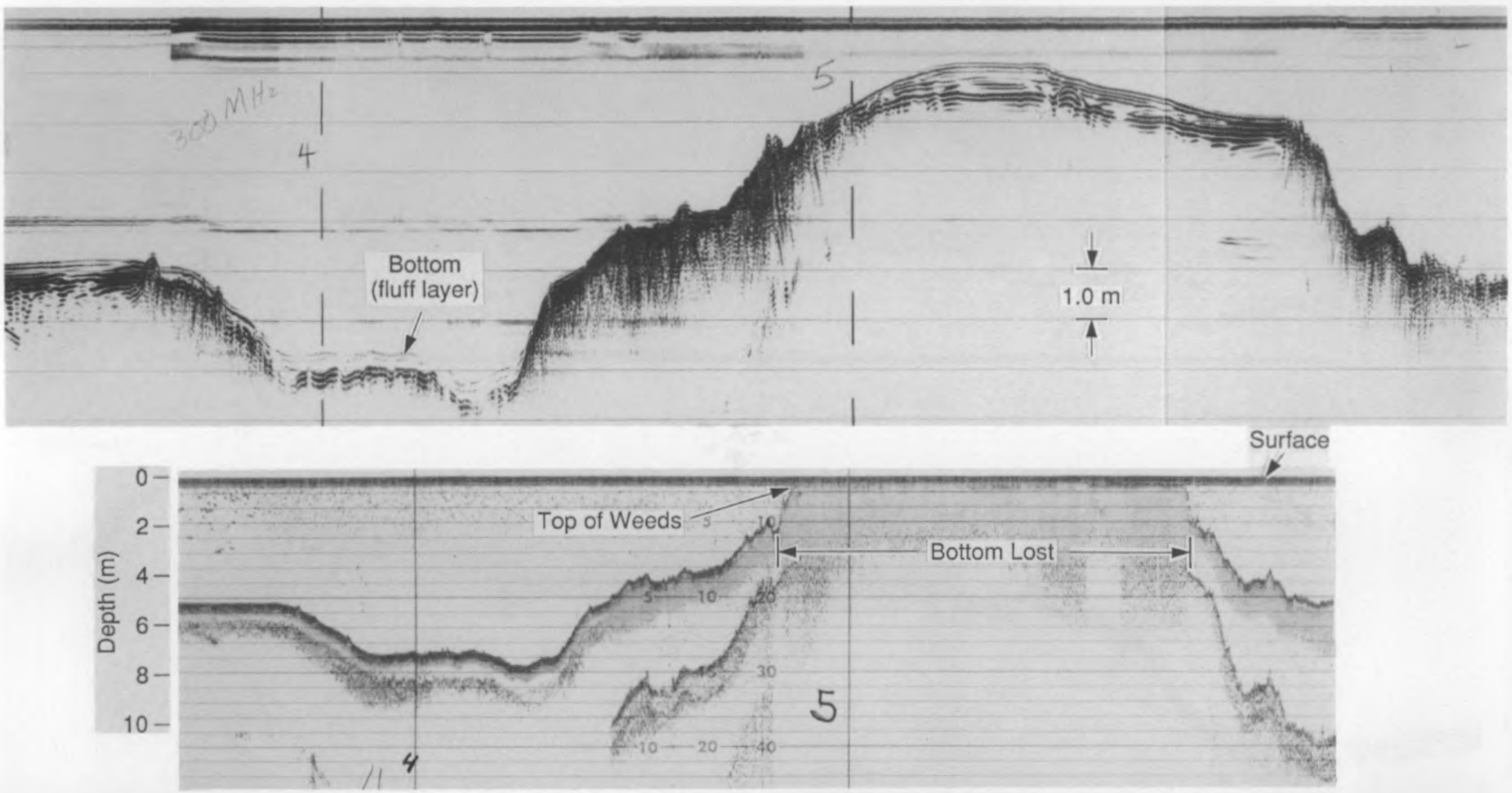

Figure 9. Radar (upper) and sonar (bottom) profiles obtained off Grass Island. The radar system not only provided the water depth over the shoal but also showed a sub-bottom layer. The so called "fluff layer" in the radar record was underlain by a strong reflector that was not detected in the sonar record.

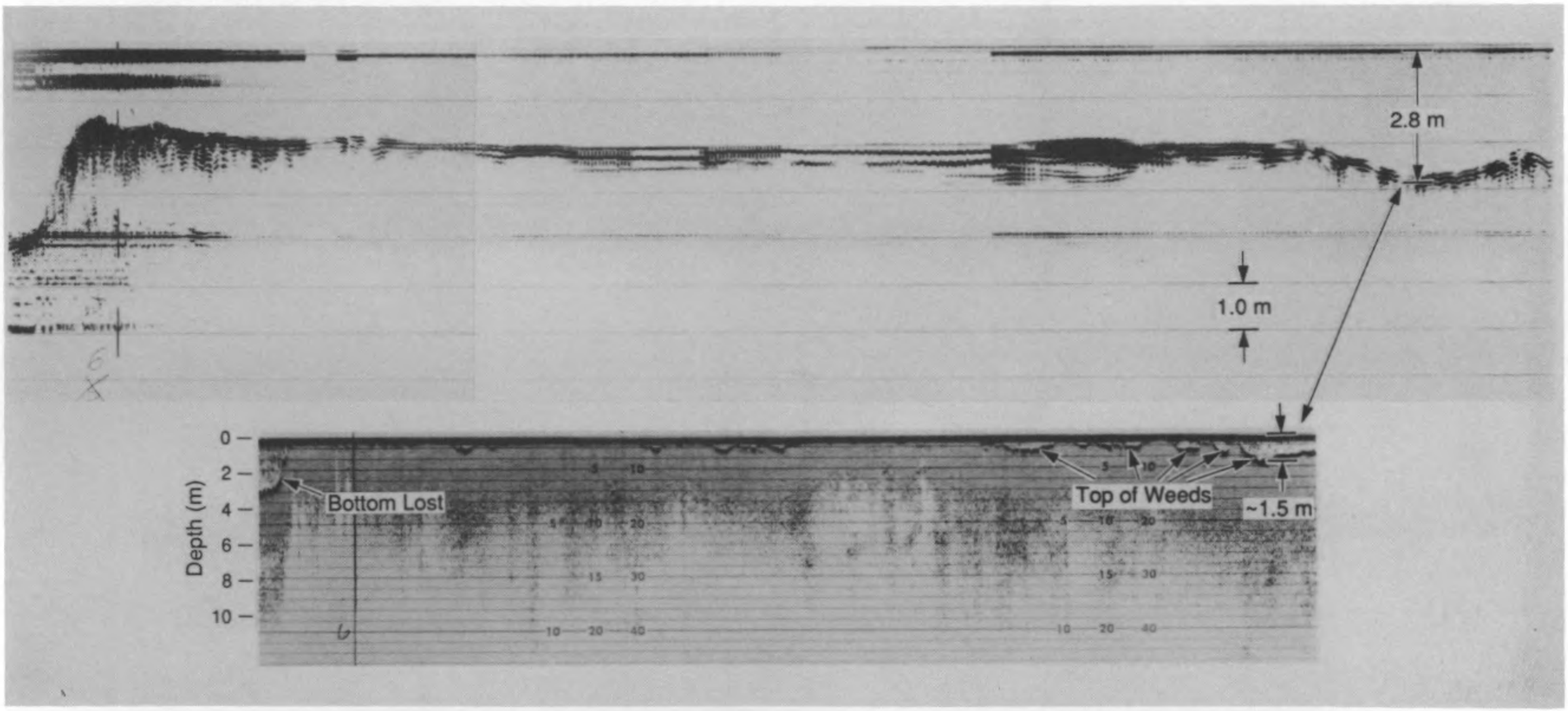

Figure 10. Radar (upper) and sonar (bottom) profiles obtained in the shallow water area off Grass Island. The sonar system again lost bottom at about the 2.5-m depth, as can be seen on the extreme left, but the system did profile the top of the vegetation "mat."

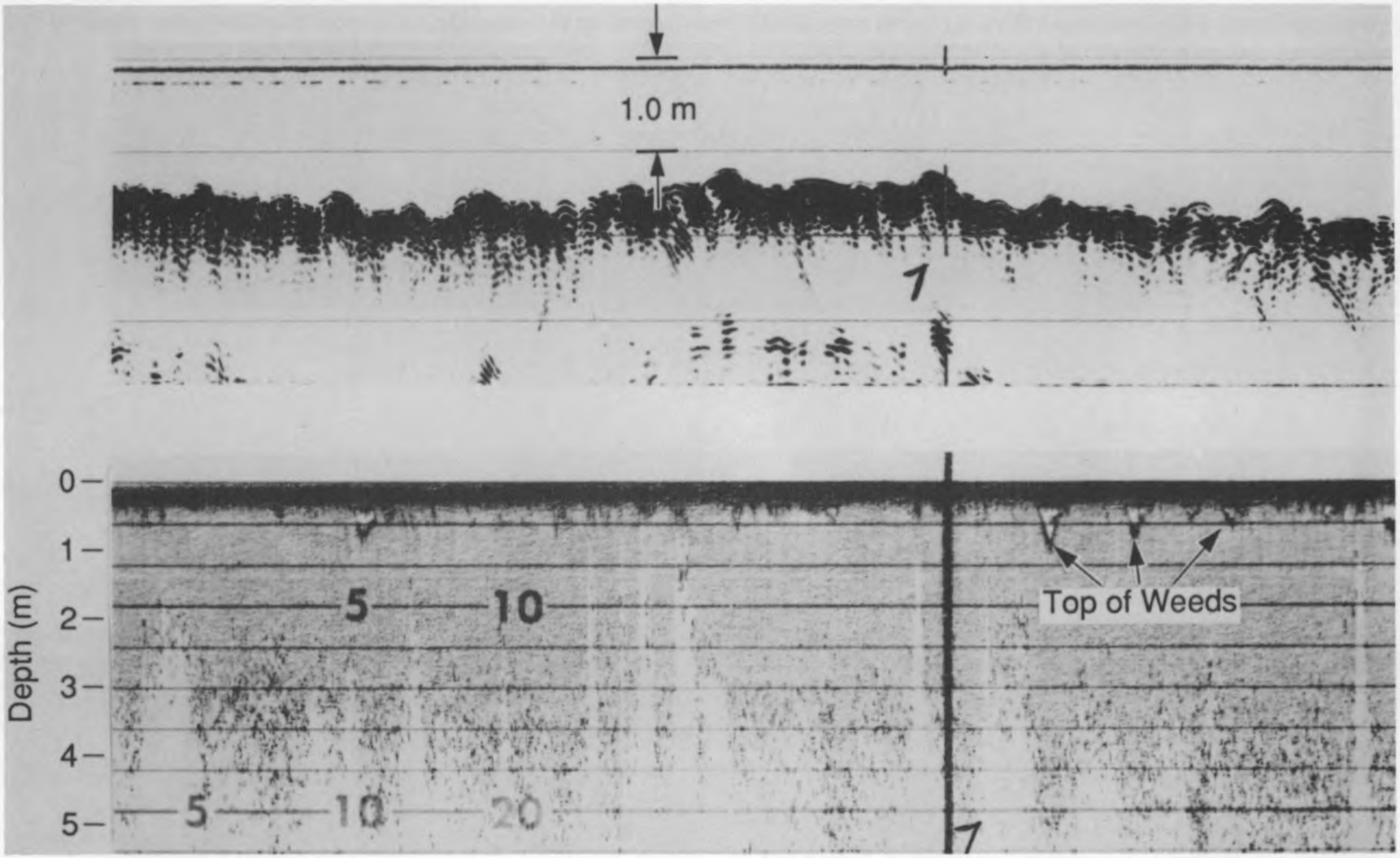

Figure 11. Radar (upper) and sonar (bottom) profiles obtained on the north side of Lake St. Francis near South Lancaster. As these records indicate, the sonar system could only profile the top of the weed layer, whereas the radar system provided good bathymetry.

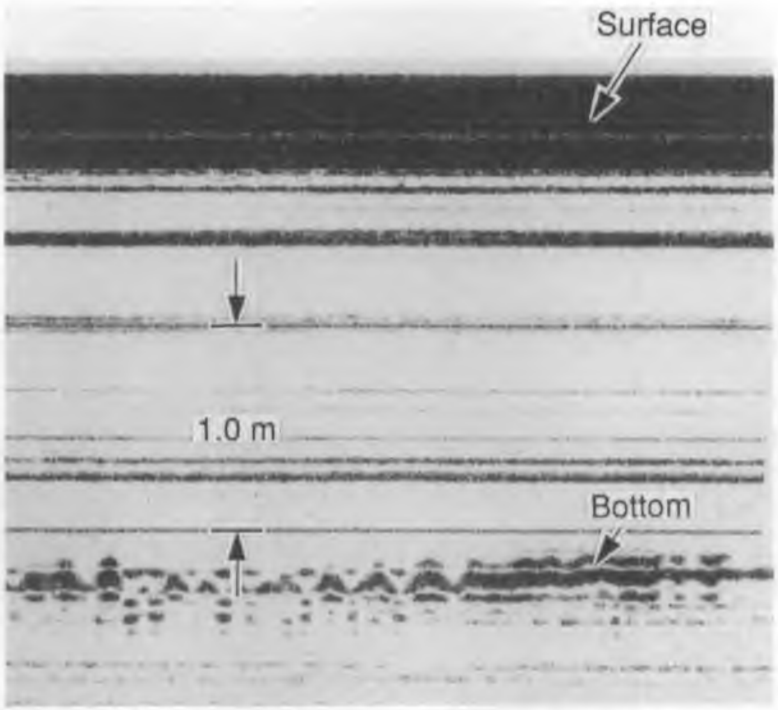

Figure 12. A through-hull bottom profile made with a 500-MHz antenna. Water is about 2.2 m deep.

In the waters near South Lancaster there was very dense weed growth. Here again the radar system, operating with the 300-MHz antenna, had no difficulty profiling the water depth, whereas the sonar system never recorded a bottom return (Fig. 11).

In this same area, the 500-MHz radar antenna (15 cm high, 30 cm wide, and 36 cm long) was placed on the floor of the survey boat, which has a double fiberglass bottom. Between the inner and outer hull is a core of foam of some unknown thickness, but it is probably 2 to 4 cm thick. Operating the radar system with the antenna in this location demonstrated that the lake bottom could be profiled through the hull of this craft (Fig. 12). The return was not as strong as when the antenna was set on the bottom of the rubber boat, but this may have been caused in part by the slanted attitude the antenna housing had to assume in the confined space available above the keel of the boat and by effects associated with antenna stand-off distance from the water.

As previously indicated in reference to the radar profile record taken in the Grass River (Fig. 8b), fish can also be detected. Another example of this is shown in Figure 13 where two apparent fish targets were recorded using the 300-MHz antenna. In March 1989, while profiling the snow plus ice thickness and the bottom of Lake Nipissing, located north of Toronto, Ontario, Canada, apparent fish targets were occasionally seen in the radar record. An example record is shown in Figure 14. This record was obtained with use of a 300-MHz antenna. Water conductivity was measured to be 4.3 mS/m in this lake. Once again, note the quality of the radar record as well as the sub-lake-bed features. The detection of fish was not surprising since Rossiter et al. (1990) have also demonstrated that impulse radar could be used to detect fish at a river fish counting station.

SUMMARY AND CONCLUSIONS

Vegetation of various types can act as an acoustic barrier or scatterer to prevent conventional sonar systems from profiling bottom topography. This was clearly demonstrated to be the case for the acoustic sonar system used in this study and for the weed conditions existing in the lakes and rivers along the St. Lawrence Seaway. The apparent bottom profiled by the acoustic sounder in the dense weed areas was actually the top of the vegetation "mat."

This demonstration study showed that impulse radar not only was capable of sounding through dense weeds to provide correct bottom profiles but also revealed shallow sub-bottom layering. Analysis of the phase, amplitude and frequency spectra of the reflected electromagnetic wavelet from the bottom could lead to a

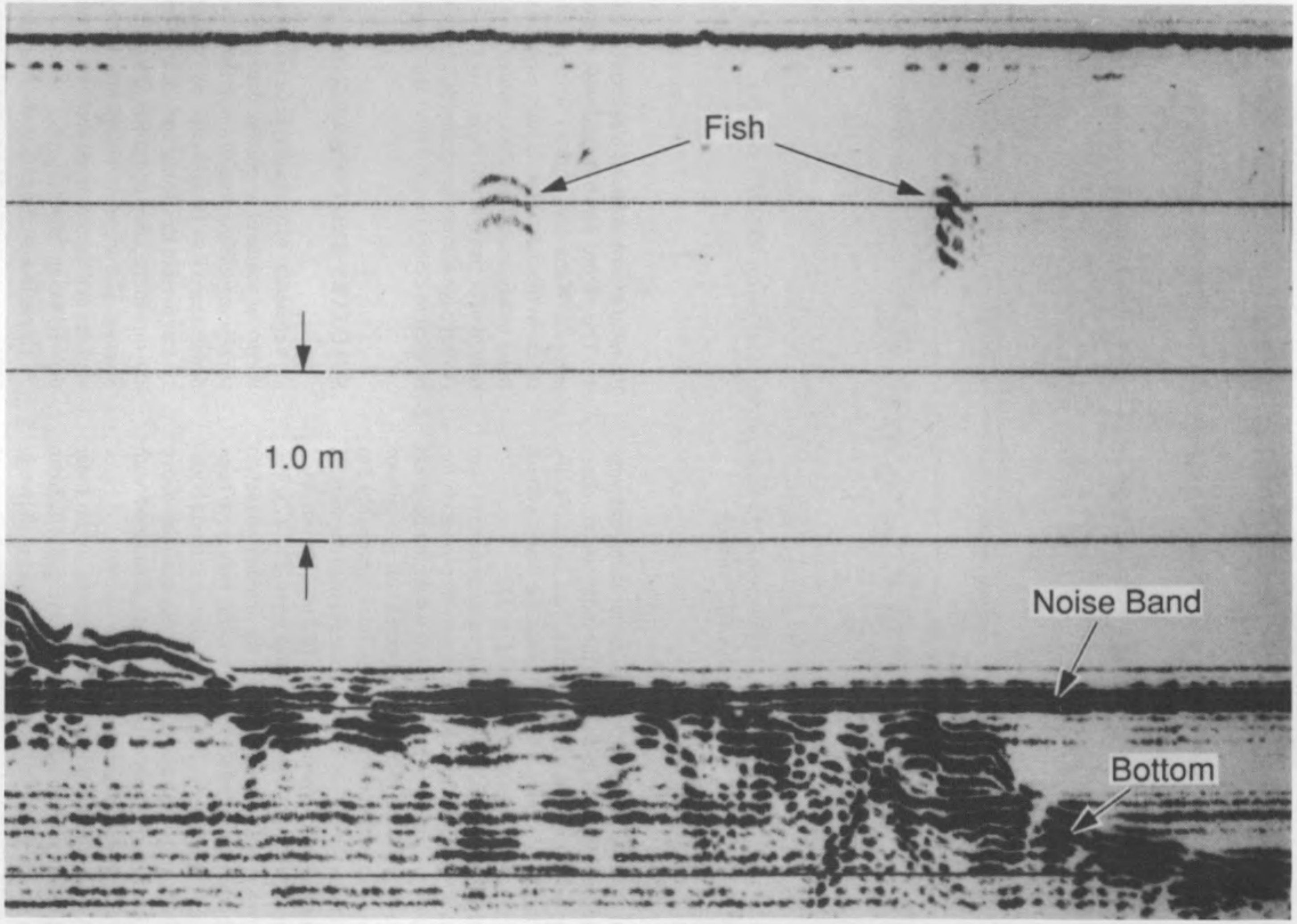

Figure 13. Fish targets in the radar profile taken near Grass Island where several fishermen were at "work."

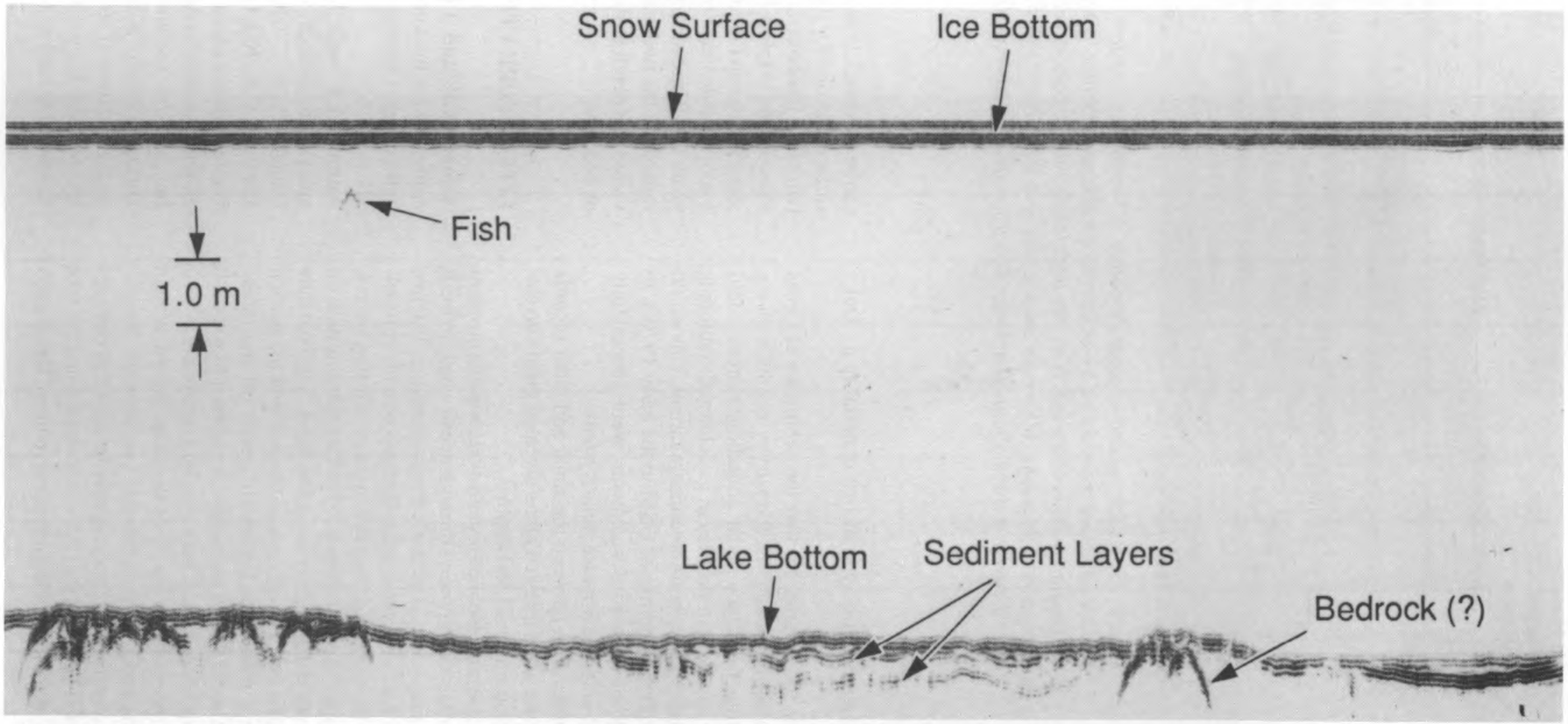

Figure 14. Radar record showing the snow plus ice thickness and the bathymetry at a Lake Nipissing site. This record was made by towing the radar antenna on the snow behind a tracked vehicle. The record covers a distance of about 300 m. Snow and ice thickness was about 0.9 m.

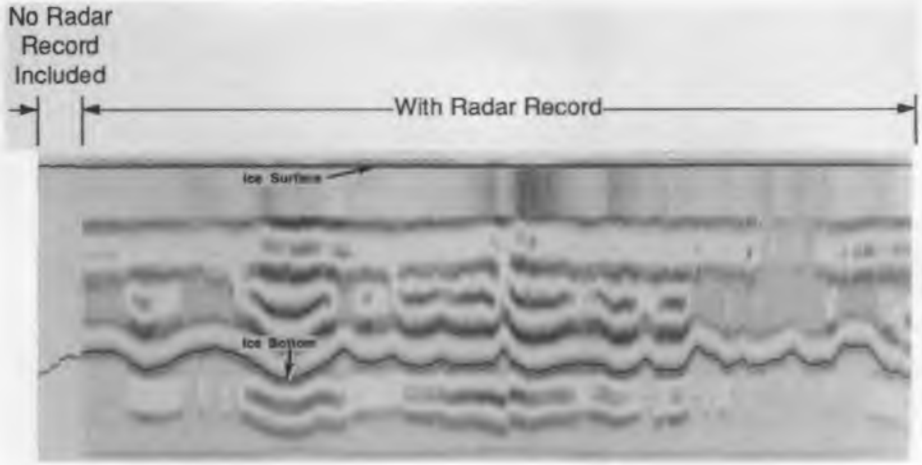

Figure 15. Radar record of approximately 1.7-m-thick snow-free sea ice. The dark, narrow bands were produced by an interface tracking algorithm. These bands represent the top and bottom of the ice. Note the undulating sea-ice bottom relief associated with snow cover variations. Where the snow cover was thick, the ice was thinner. The radar record covers a track about 80 m long (Kovacs, unpublished record).

determination of the type of bed material (e.g., Duke 1990).

Under the assumption that the sediments at Grass Island had gas inclusions, the survey results indicate that a low frequency radar sounding system could provide sub-bottom profiles in gas charged sediments where acoustic sub-bottom sounders cannot. This would agree with the findings of GSSI in the early 1970's, in which known gaseous sediments were successfully sounded using an impulse radar system.

A comparison between the sonar and radar records outside the weed infested areas revealed good correlation in bottom detail and depth.

Impulse radar technology can overcome the problem of not being able to sound through dense weeds in fresh water using standard acoustic depth sounding systems. However, a conveyance other than a boat with a propeller will be needed for surveys in weed-infested waters. The propeller of the boat used in this test did pick up weeds, which had to be removed by hand. A jet boat may work but it may require special screens over the suction inlet or a method to backflush weeds off the intake screen should this be necessary. An airboat or a special hovercraft-type vessel may also be appropriate.

To improve the display of the radar record, certain real-time processing of the data can be done. For example, a correlation function may be used that captures a reflected wavelet from the water surface and the lake bottom and then tracks these two returns. The display can be two black lines on the graphic record, one for the surface and one for the bottom, or a display where the two black lines overlay the radar record. The former is shown at the extreme left and the latter in the remaining record shown in Figure 15. This real-time record shows a short profile made on sea ice by the author nearly 10 years ago. The distance between the two lines of course represents the two-way flight time, which can be converted to a depth or digitally recorded for later plotting as needed.

LITERATURE CITED

Annan, A.P. and J.L. Davis (1977a) Impulse radar applied to ice thickness measurements and freshwater bathymetry. Geological Survey of Canada, Paper 77-1B, p. 63–65.

Annan, A.P. and J.L. Davis (1977b) Radar range analysis for geological materials. Geological Survey of Canada, Paper 77-1B, p. 117–124.

Bertram, C.L., K.J. Campbell and S.S. Sandler (1972) Characteristics of sea ice, lake ice and permafrost using an impulse radar system. Geophysical Survey Systems Inc., Internal Technical Report No. 008-72.

Duke, S. (1990) Calibration of ground penetrating radar and calculation of attenuation and dielectric permittivity. Masters Thesis (unpublished). Golden, Cororado: Colorado School of Mines.

Kovacs, A. and G. Abele (1974) Crevasse detection using an impulse radar system. *Antarctic Journal of the United States,* **9**(4): 175–178.

Kovacs, A. and A.J. Gow (1975). Brine infiltration in the McMurdo Ice Shelf, McMurdo Sound, Antarctica. *Journal of Geophysical Research,* **80**(15): 1957–1961.

Kovacs, A. (1977a) Iceberg thickness and crack detection. *First International Conference and Workshops on Iceberg Utilization, Iowa State University of Science and Technology, Ames, Iowa,* p. 131–145.

Kovacs, A. (1977b) Sea ice thickness profiling and under ice oil entrapment. In *Proceedings of the 9th Annual Offshore Technology Conference, Houston, Texas.* OTC Paper 2949, p. 549–554.

Kovacs, A. (1978) Remote detection of water under ice-covered lakes on the North Slope of Alaska. *ARCTIC,* **31**(4): 448–458.

Kovacs, A. and R.M. Morey (1979) Remote detection of a freshwater pool off the Sagavanirktok River delta, Alaska. *ARCTIC,* **32**(2): 161–164.

Kovacs, A. and R.M. Morey (1980) Investigations of sea ice anisotropy, and electromagnetic properties, strength, and under-ice current orientation. USA Cold Regions Research and Engineering Laboratory, CRREL Report 80-20.

Kovacs, A. and R.M. Morey (1985) Impulse radar sounding of frozen ground. In Workshop on permafrost geophysics (J. Brown, M.C. Metz and P. Hoekstra, Eds.). USA Cold Regions and Research and Engineering Laboratory, Special Report 85-5, p. 28–40.

Kovacs, A. (1990) Investigation of the L1Z-3 Dew Line Station Water Supply Lake. USA Cold Regions and Research and Engineering Laboratory, CRREL Report 90-11.

Morey, R., A. Orange and K. Campbell (1973) Application of electromagnetic subsurface profiling to the study of permafrost. Geophysical Survey Systems Inc. Internal Report No. 0133.

Orange, A. K. Campbell and W. Corrieri (1973) Sea ice thickness determination using electromagnetic subsurface profiling. Geophysical Survey Systems Inc., Internal Report No. 0144.

Rossiter, J.R., E. Reimer, L.A. Lalumiere and D.R. Inkster (1990) Radar cross-section of fish at VHF. Workshop on Ground Penetrating Radar. Geological Survey of Canada, Paper 90-4.

Smith, G.S. (1984) Directive properties of antennas for transmission into a material halfspace. *IEEE Transactions, Antennas and Propagation,* AP-32, p. 232–246.

Smith, G.S. and Scott, W.R. (1989) A scale model for studying ground penetrating radars. *IEEE Transactions on Geoscience and Remote Sensing,* **27**(4): 358–363.

Ulriksen, C.P.F. (1986) Ice thickness measurements with airborne impulse radar. Lund University of Science and Technology, Lund, Sweden, Report TVTG-3012.

Wensink, W.A., G. Greeuw, J. Hofman and J.K. VanDeen (1990) Measured underwater near-field E-patterns of a pulsed, horizontal dipole antenna in air: comparison with the theory of the continuous wave, infinitesimal electric dipole. *Geophysical Prospecting,* **38:** 805–830.

REPORT DOCUMENTATION PAGE

Form Approved
OMB No. 0704-0188

1. AGENCY USE ONLY (Leave blank)	2. REPORT DATE	3. REPORT TYPE AND DATES COVERED
	April 1991	

4. TITLE AND SUBTITLE

Impulse Radar Bathymetric Profiling in Weed-Infested Fresh Water

5. FUNDING NUMBERS

6. AUTHORS

Austin Kovacs

7. PERFORMING ORGANIZATION NAME(S) AND ADDRESS(ES)

U.S. Army Cold Regions Research and Engineering Laboratory
72 Lyme Road
Hanover, N.H. 03755-1290

8. PERFORMING ORGANIZATION REPORT NUMBER

CRREL Report 91-10

9. SPONSORING/MONITORING AGENCY NAME(S) AND ADDRESS(ES)

10. SPONSORING/MONITORING AGENCY REPORT NUMBER

11. SUPPLEMENTARY NOTES

12a. DISTRIBUTION/AVAILABILITY STATEMENT

Approved for public release; distribution is unlimited.

Available from NTIS, Springfield, Virginia 22161.

12b. DISTRIBUTION CODE

13. ABSTRACT (*Maximum 200 words*)

An evaluation of an impulse radar sounding system for profiling bottom topography in weed-infested waters is discussed. Field results are presented comparing radar profiles of water depth with those obtained with a conventional acoustic depth sounder. It was found that the impulse radar system could profile freshwater depths through dense vegetation, whereas the acoustic depth sounder could not.

14. SUBJECT TERMS

Acoustic sounding, Depth sounding, Impulse radar, Bathymetry, Fresh water sounding

15. NUMBER OF PAGES

26

16. PRICE CODE

17. SECURITY CLASSIFICATION OF REPORT	18. SECURITY CLASSIFICATION OF THIS PAGE	19. SECURITY CLASSIFICATION OF ABSTRACT	20. LIMITATION OF ABSTRACT
UNCLASSIFIED	UNCLASSIFIED	UNCLASSIFIED	UL

NSN 7540-01-280-5500

Standard Form 298 (Rev. 2-89)
Prescribed by ANSI Std. Z39-18
298-102